Materials Today Bio 25 (2024) 101003

Contents lists available at ScienceDirect

Materials Today Bio

journal homepage: www.journals.elsevier.com/materials-today-bio

Fabrication of bioengineered corneal endothelial grafts using an allogeneic cornea-derived matrix

Lijie Xie [a,b], Xiaojuan Dong [b], Jianping Ji [b], Chen Ouyang [b], Jing Wu [b], Chao Hou [b], Ting Huang [b,*]

[a] Guangdong Eye Institute, Department of Ophthalmology, Guangdong Provincial People's Hospital (Guangdong Academy of Medical Sciences), Southern Medical University, Guangzhou, China
[b] State Key Laboratory of Ophthalmology, Zhongshan Ophthalmic Center, Sun Yat-sen University, Guangzhou, China

ARTICLE INFO

Keywords:
Allogeneic cornea-derived matrix
Biomimetic reconstruction
Corneal endothelial cells
Descemet membrane endothelial keratoplasty

ABSTRACT

Corneal endothelial keratoplasty has been the primary treatment method of endothelial decompensation, but it is often limited in clinical practice due to global shortage of donor cornea. Here, we explored using an ultra-thin allogeneic cornea-derived matrix (uACM) films as a substrate for constructing bioengineered corneal endothelial grafts. We evaluated the films' optical, mechanical, and structural properties, and measured the composition of the extracellular matrix. The uACM was an ultrathin and curved cornea-shaped film with favorable optical and mechanical properties. The fabrication process efficiently preserved corneal extracellular matrix composition and significantly decreased cellular components. Moreover, human corneal endothelial cells and rabbit corneal endothelial cells (RCECs) can adhere and grow on the uACM films with a positive expression of the corneal endothelial functional markers Na^+/K^+-ATPase and ZO-1. The successful transplantation of uACM with RCECs grafts into the rabbit model of endothelial dysfunction via Descemet membrane endothelial keratoplasty resulted in prompt restoration of corneal transparency and thickness. During the four-week follow-up period, the uACM with RCECs implanted eyes exhibited comparable corneal transparency, central corneal thickness, and endothelial cell count to that of the healthy rabbit. Histologic examination revealed that the grafts were successfully attached and integrated onto the posterior surface of the corneal stroma. The uACM achieved biomimetic reconstruction in terms of both composition and structure, and can be used to construct the bioengineered corneal endothelial grafts. These results indicate that constructing bioengineered corneal endothelial grafts from discarded human corneal tissues may pave the way for generating high-quality corneal endothelial grafts for transplantation.

1. Introduction

The cornea is the transparent outmost layer of the eyeball. The corneal endothelium, which resides on the inner surface of the cornea, is responsible for maintaining corneal transparency through the pump and barrier functions of human corneal endothelial cells (HCECs) [1]. The density of HCECs gradually decreases at a rate of 0.3–0.6% per year with normal aging. Due to the limited proliferative capacity in vivo, the cells attempt to compensate by increasing the cell enlargement and migration [2]. Various factors can lead to the loss of HCECs and corneal decompensation, including degenerative aging, endothelial dystrophy, intraocular surgery, and inflammation. When the endothelial cell numbers are distinctly reduced, the cornea will lose its transparency, leading to blindness [1,3].

Currently, corneal blindness is usually caused by endothelial dysfunction and restored vision by corneal transplantation surgery [4,5]. In the past two decades, significant progress has been achieved in corneal endothelial transplantation. The surgical techniques of corneal

Abbreviations: uACM, ultra-thin allogeneic cornea-derived matrix; RCECs, rabbit corneal endothelial cells; HCECs, human corneal endothelial cells; PK, penetrating keratoplasty; EK, endothelial keratoplasty; DMEK, Descemet membrane endothelial keratoplasty; ECM, extracellular matrix; LK, lamellar keratoplasty; ACM, allogeneic cornea-derived matrix; OD, Optical density; SEM, scanning electron microscopy; TEM, transmission electron microscopy; AS-OCT, Anterior segment-optical coherence tomography; CCT, central corneal thickness; SD, standard error; GO, Gene Ontology.

* Corresponding author.
E-mail address: thuang@vip.163.com (T. Huang).

https://doi.org/10.1016/j.mtbio.2024.101003
Received 29 November 2023; Received in revised form 13 February 2024; Accepted 15 February 2024
Available online 22 February 2024

endothelial dysfunction have evolved from penetrating keratoplasty (PK) to endothelial keratoplasty (EK), which only replaces Descemet's membrane and endothelial cell layer instead of full-thickness cornea [6–8]. Fuchs' endothelial dystrophy is the main corneal transplantation surgery indication, accounting for about 39% of the global corneal transplantation surgery [9]. Descemet membrane endothelial keratoplasty (DMEK) has been the primary treatment method of endothelial decompensation, but it is often limited in clinical practice due to the global shortage of donor cornea [10–12]. Hence, there is an immediate requirement for donor cornea substitutes that possess exceptional endothelial function to adequately address clinical needs. Bioengineered corneal endothelial grafts offer a potential solution to the scarcity issue [13–16].

The optimal corneal endothelial graft should exhibit excellent physiochemical properties, biocompatibility, endothelial function, and the ability to withstand the in vivo EK surgical procedure. In previous studies, the corneal endothelial scaffold can be classified into natural, synthetic, and composite materials. Natural materials mainly include amniotic membrane, Descemet's membrane, anterior lens capsule, acellular corneal stroma, and silk fibroin membrane, which contain a variety of cytokines and have good biocompatibility. Despite those significant advantages, there are clear disadvantages associated with poor optical and mechanical properties, and the scarcity of donor cornea. Synthetic materials have a wide range of sources, and the fabrication process can control the physicochemical properties. Still, they are often limited by their poor biocompatibility and the unknown metabolic process in vivo. The natural corneal stromal layer has a unique extracellular matrix (ECM) composition in the microenvironment of corneal cell growth. Using ECM as a raw material to reconstruct bioengineered corneal endothelial scaffolds has incomparable advantages over other materials from the perspective of composition bionics. In the clinic, a large amount of residual donor corneal tissue after allogeneic keratoplasty is clinically discarded, including the residual peripheral corneal portion after PK, the remanent posterior lamellar tissue after lamellar keratoplasty (LK), and the remaining anterior lamellar tissue after EK. Our previous research has provided evidence supporting the feasibility and potential of utilizing discarded human corneal tissues to create allogeneic cornea-derived matrix (ACM) scaffolds for corneal stromal implants. The ACM scaffolds displayed favorable optical properties and structural strength, featuring ECM components similar to those of human corneal stroma [17]. Thus, we considered the prospect of developing bioengineered corneal endothelial grafts using ACM, aiming to closely mimic the composition and structure of the human corneal endothelium and thereby restore the original tissue's functionality.

We explored the use of residual corneal tissue discarded after allogeneic corneal transplantation to construct the ultra-thin allogeneic cornea-derived matrix (uACM) films, and then cultured HCECs and RCECs on the surface of the films to fabricate bioengineered corneal endothelial grafts. Furthermore, the endothelial grafts were surgically implanted using DMEK surgery in a rabbit model of corneal endothelial decompensation to assess their biocompatibility in vivo. The objective of the present study was to develop and implement a novel and effective alternative corneal endothelial graft for the treatment of corneal endothelial keratopathy.

2. Materials and methods

2.1. Preparation of uACM films

The study followed the tenets of the Declaration of Helsinki. The human corneal tissue was provided by the Eye Bank of Guangdong Province, China. The decellularized human corneal tissue suspension was fabricated according to our previously described method [17]. We collected discarded human corneal tissues from allogeneic corneal transplantation surgery and then repeated freeze-thaw three times to achieve the human corneal tissue suspension. The decellularization process was applied and immediately freeze-dried to achieve the lyophilized powder that was blended with ultrapure water at a concentration of 5 mg/mL using a homogenizer. About 200 μL of the homogenized corneal tissue suspension was added to the spherical mold with a curvature radius of 8 mm and then air-dried at a constant temperature (26 °C) and humidity (75–85%) to form the uACM films.

2.2. Optical analysis

The dry and pre-wet films (immersed in PBS solution for 24 h) were positioned on the surface of a transparent ruler to facilitate transparency observation and photographic documentation.

2.3. Mechanical testing

The uACM film was cut into dumbbell-shaped sample strips with a length of 4 mm and a width of 5 mm. Tensile strength, elongation at break, and elastic modulus of the dry and pre-wetted uACM films were subjected to tensile tests using a Model 3342 tensile testing machine (Instron, USA) with a tensile rate of 0.1 mm/s. The thickness of the samples was measured with a digital thickness gauge, with an accuracy of 1 μm.

2.4. Histochemistry

The normal donor cornea and uACM films were paraformaldehyde-fixed and embedded in paraffin. Sections (5-μm-thick) were stained with H&E for the global structure, Picrosirius red for global collagens, Periodic acid-Schiff kit for global glycoproteins, and Alcian blue for global glycosaminoglycans.

2.5. Mass spectrometry-based proteomics

Protein extraction and iTRAQ experiments were performed using a modification of a previously standard proteomics methods [18]. Briefly, four paired samples (10 mg dry weight each) of donor cornea and uACM films were prepared and used for a phenol protein extraction procedure, and the protein concentrations were determined using the Bradford colorimetric method. Total protein (100 μg) underwent acetone precipitation, followed by re-dissolution in 500 mM triethylammonium bicarbonate and the addition of 5 μg trypsin (Beijing Hualishi Technology, China). The resulting digested peptides were incubated at 37 °C for 4 h, desalted, and freeze-dried. The peptides were labeled with 8-plex iTRAQ reagents (Applied Biosystems, USA) in accordance with the manufacturer's instructions. After labeling, the samples were combined and lyophilized. The iTRAQ-labeled peptides that had been dried were subjected to prefractionation through offline Strong Cation Exchange chromatography, utilizing the LC-20AB HPLC Pump system (Shimadzu, Japan). The reconstituted dried peptide fractions were then subjected to analysis using LC-MS/MS on the UltiMate 3000 UHPLC system (Thermo, USA). Following liquid phase separation, the peptides were ionized using a nanoESI source and subsequently introduced into the Q Exactive HF-X tandem mass spectrometer (Thermo, USA) for detection through data-dependent acquisition. The raw mass spectrometry data were then searched for identification by comparing them to the Swissprot database with the Mascot software (version 2.3.02). Quality control analysis was also performed to determine whether the data were acceptable. Quantitative analysis of the iTRAQ data was performed using the IQuant software (BGI, Shenzhen, China) [19]. The final differential proteins were screened with fold change >1.2 and P-value <0.05.

2.6. DNA quantification

The normal donor cornea and uACM films were lyophilized and weighed. DNA micro-extraction kit (QIAGEN, Germany) was used

according to the instructions to extract DNA, and then the DNA content was determined using the NanoDrop One micro-ultraviolet spectrophotometer (Thermo, USA).

2.7. Scanning electron microscopy and transmission electron microscopy imaging

For scanning electron microscopy (SEM), uACM films were fixed in 2.5% glutaraldehyde at 4 °C for 4 h, followed by post-fixation in 1% osmium tetroxide in 0.1 M phosphate buffer. Samples were dehydrated with a graded ethanol series and placed in isoamyl acetate, then moved to a critical point dryer. Observation of films' surface morphology and fiber morphology under U8010 scanning electron microscope (HITACHI, Japan). For transmission electron microscopy (TEM), uACM films and donor cornea were fixed in 2.5% glutaraldehyde at 4 °C for 4 h, followed by post-fixation in 1% osmium tetroxide in 0.1 M phosphate buffer. Samples were dehydrated with a graded series of ethanol and embedded in epoxy resin. The 60–80 nm sections were stained with uranyl acetate and lead citrate. Observations were carried out by HT7700 transmission electron microscope (HITACHI, Japan). The mean fiber diameter was determined using twenty fibers randomly observed on the TEM images and calculated by ImageJ 1.52 software.

2.8. Isolation and culturing of corneal endothelial cells

HCECs and rabbit corneal endothelial cells (RCECs) were achieved according to previous studies [20,21]. Briefly, CECs clusters were isolated through 1 mg/mL Collagenase A for 2–4 h and then treated with TrypLE Express for 5–10 min to create a single-cell suspension. Isolated CECs were seeded onto the FNC coating mix (AthenaES, USA) pre-coated plates at a density of 1.0×10^4 cells/cm^2 and cultured on stabilization medium (Human Endothelial-SFM supplemented with 5% serum) overnight. Subsequently, CECs were cultured in the proliferative medium (Ham's F12/M199 supplemented with 5 % serum, 20 μg/mL ascorbic acid, 1x ITS, and 10 ng/mL HrFGF) to promote the proliferation of the attached CECs for seven to fourteen days until cells reached 90% confluence. CECs were re-cultured in the stabilization medium for two days before being sub-cultured via single-cell dissociation using TrypLE Express. Isolated CECs were sub-cultured at a density of 1.0×10^4 cells/cm^2 on the precoated plate for further expansion.

2.9. Preparation of bioengineered corneal endothelial graft

Primary HCECs and RCECs from three passages were seeded onto the posterior surface of uACM films at a density of 3000 cells/cm^2. These cells were then maintained in the stabilization medium for a duration of 7 days to generate bioengineered human and rabbit corneal endothelial grafts. Subsequently, the grafts were preserved in a Corneal storage medium (Alchimia, Italy) for a short-term until further experiments.

2.10. Immunocytochemistry

2.10.1. Immunocytochemistry staining

The human corneal endothelium, rabbit corneal endothelium, human corneal endothelial grafts, and rabbit corneal endothelial grafts were fixed in pre-cooled 100% methanol for a duration of 10 min at a temperature of −20 °C. Subsequently, permeabilization was carried out using 0.3% Triton X-100 for a period of 15 min at room temperature. Following this, the samples underwent three consecutive 5-min rinses with PBS. The samples were then exposed to a blocking buffer consisting of PBS with 10% donkey serum and 0.3% Triton X-100 for a duration of 1 h at room temperature. After overnight incubation at 4 °C with anti-Na^+/K^+-ATPase (Santa cruz, USA) and anti-ZO-1 (Thermo, USA), the samples were washed with PBS and incubated in the corresponding secondary antibodies (1:300, Jackson) for 1 h at room temperature. Nuclei were stained with DAPI and washed twice with PBS for 5 min each. The expression of Na^+/K^+-ATPase and ZO-1 on the surface of the samples was observed under a laser scanning confocal microscope and photographed.

2.10.2. Live-dead viability assay

The rabbit corneal endothelial grafts were removed from the corneal storage medium, rinsed with sterile PBS, and flattened under a dissecting microscope for corneal spreading. The LIVE/DEAD Viability/Cytotoxicity Assay Kit (Thermo, USA) was prepared into 4 mM calcein AM and 2 mM ethidium homodimer (EthD-1) with PBS solution and incubated in the dark for 30 min for live-dead cell staining. Cells were observed simultaneously under a laser-scanning confocal microscope.

2.11. EK surgical procedure

All animal operations were performed according to the requirements of the Association for Research in Vision and Ophthalmology (ARVO) Statement, and were approved by the Animal Ethics Committee of Zhongshan Ophthalmology Center of Sun Yat-sen University. New Zealand white rabbits of either gender weighing 2–3 kg were randomly divided into three groups: uACM with RCECs transplantation group (the rabbit corneal endothelial grafts were transplanted after stripping the Descemet's membrane, n = 5), uACM without RCECs transplantation group (uACM films were transplanted after stripping the Descemet's membrane, n = 5), Descemetorhexis group (stripping the Descemet's membrane without transplantation, n = 5). One operator performed all operations. The right eye of all experimental animals was selected as the surgical eye. General anesthesia was performed by intramuscular injection of 3% sodium pentobarbital. The 10-mm diameter Descemet's membrane and the endothelial layer of the rabbit cornea were dissected to establish the corneal endothelial dysfunction animal model. Trypan blue staining was used to show the peeled area, and then the filtered air was injected into the anterior chamber. The uACM with RCECs grafts were stained with Trypan blue, cut with an 8-mm diameter corneal trephine, and curled autonomously into the DMEK injector. The grafts were implanted into the anterior chamber by a DMEK injector through a corneal incision and adjusted to achieve the endothelial surface face down and in the central cornea. Finally, the grafts were fixed to the posterior surface of the rabbit corneal stroma by air injection into the anterior chamber. After the operation, the surgical animal was placed in a warm and quiet place, and the surgery eye was placed on the upper side for half an hour until it woke up. Tobramycin eye ointment three times a day during the first week and tobramycin dexamethasone eye drops three times a day during the second to fourth weeks.

2.12. Post-transplantation examination

Corneal imaging and measurements were performed at 1 day, 4 days, 1 week, 2 weeks, 3 weeks, and 4 weeks postoperatively. Slit-lamp photographs were used to evaluate corneal transparency, graft adhesion, and anterior chamber inflammatory reaction. The corneal transparency score of the implanted cornea was performed according to the previous article [22]. To assess the graft's adherence to the posterior corneal stroma and measure the central corneal thickness, Anterior segment-optical coherence tomography (AS-OCT; Heidelberg, Germany) was employed. The central corneal thickness (CCT) was averaged at the three positions of center (0 mm), +1.0 mm, and −1.0 mm on both sides of the center. In cases where the central corneal thickness surpassed the maximum measurable depth, rendering its calculation unfeasible, a value of 1900 μm was recorded. The corneal endothelial count was counted by a specular microscope SP-3000P (TOPCON, Japan), and enface corneal thickness was measured by a corneal topography (Allegro Oculyzer, Germany). Four weeks after surgery, the corneas were harvested and rinsed with PBS solution. HE staining was performed to show the adhesion of the grafts to the transplanted rabbit corneas. Immunohistochemical staining with an antibody against

Na^+/K^+-ATPase, ZO-1, and N-Cadherin was used to identify characteristic markers of CECs in the transplanted rabbit corneas. SEM imaging was conducted to evaluate the microscopic morphology of CECs on the transplanted rabbit corneas.

2.13. Statistical analysis

The data were expressed as mean ± standard error (SD). GraphPad Prism software (Version 8.2.0, GraphPad Software, Inc.) was used for statistical analysis and data processing. One-way ANOVA was used for comparison among them. $P < 0.05$ was considered statistically significant (*$P < 0.05$, **$P < 0.01$, ***$P < 0.001$).

3. Results

3.1. Physical characterization

Fig. 1A shows the appearance of the uACM films. The transparency of the dry films was poor, while the pre-wet films had excellent transparency. The Young's modulus, elongation at break, and ultimate strength were calculated by the stress-strain curve (Fig. 1B). As can be seen from Table 1, all indexes of the films under different hydration states showed statistical differences ($P < 0.05$). The thickness of the dry film was 7.27 ± 1.20 μm, and the pre-wet film was 20.20 ± 2.52 μm. The tensile strength of the dry film (14.44 ± 0.96 MPa) was higher than that of the wet film (0.17 ± 0.03 MPa). The hydration of the films increased the elongation at break, with average values of 6.18 ± 0.92% and 9.04 ± 0.88% for the dry and wet uACM films, respectively. The Young's modulus of the uACM film after saturated water absorption decreased from 319.93 ± 17.74 MPa to 2.59 ± 0.13 MPa.

3.2. Extracellular matrix composition preservation

H&E staining showed that the uACM film had a complete and continuous structure, and no cells remained. PAS staining, Alcian blue staining, and Sirius red staining showed that the donor corneal extracellular matrix's glycoprotein, glycosaminoglycan, and collagen components were successfully retained in the uACM (Fig. 2A). Mass spectrometry iTRAQ was used to detect the relative expression of proteins in the donor cornea and uACM film. By Gene Ontology (GO) subcellular localization analysis of the significantly down-regulated differential proteins, it was found that most (97.2%) proteins removed in this study belonged to cellular components (Fig. 2B), while various types of collagens, fibronectin, and laminin in the extracellular matrix was preserved (Fig. 2C). The DNA content in the donor cornea was 166.49 ± 32.65 ng/mg, and in the uACM film was 5.83 ± 0.56 ng/mg, and there was a statistically significant difference between the two groups.

Table 1
Mechanical properties of the uACM films.

	Thickness (μm)	Tensile strength (MPa)	Elongation at break (%)	Young's modulus (MPa)
Dry Films	7.27 ± 1.20	14.44 ± 0.96	6.18 ± 0.92	319.93 ± 17.74
Prewet Films	20.20 ± 2.52	0.17 ± 0.03	9.04 ± 0.88	2.59 ± 0.13
Descemet's membrane [23]		0.3 ± 0.01	1.7 ± 0.2	2.6 ± 0.4

3.3. Microstructural characterization

Scanning electron microscope showed that the microstructures of the anterior and posterior surfaces of the uACM film were diffusely distributed collagen fibrous structures and connected densely. The stromal layer of the donor cornea (after femtosecond laser ablation) showed loosely distributed fibrous structures with a regular shape (Fig. 3A). Under the transmission electron microscope observation, the collagen fiber structure in the cross-section of the uACM film was clear,

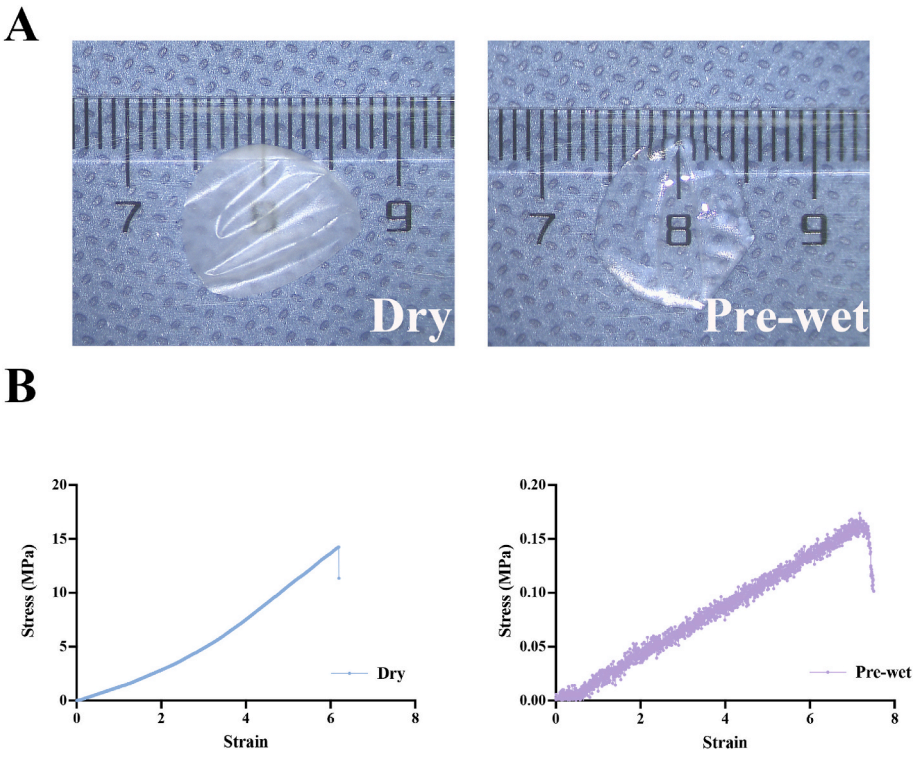

Fig. 1. Optical transparency and mechanical properties of the uACM. (A) Gross view of the dry and pre-wet uACM films. (B) Stress curve of dry and pre-wet uACM films.

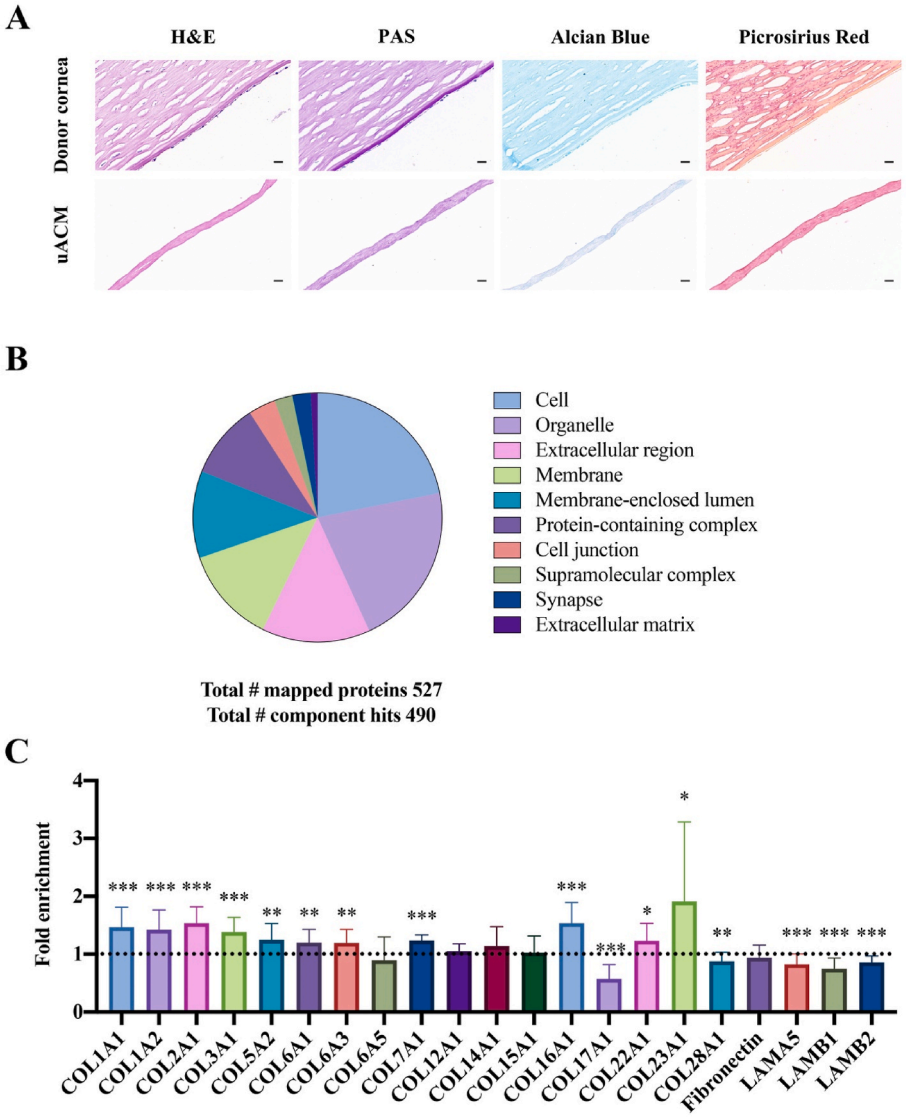

Fig. 2. Composition of the uACM. (A) Histochemical staining of donor corneas and uACM films. Scale bar = 20 μm. (B, C) Proteomic analysis of donor corneas and uACM films. (B) Subcellular localization of significantly reduced proteins after the fabrication process based on GO analysis. Percentage is shown as gene hits against total component hits. (C) The major ECM proteins like collagens and fibronectin were largely unaffected by the fabrication process.

and the fiber arrangement was similar to that of the donor corneal stroma (Fig. 3B). There was no significant difference in the diameter of collagen fibers between the two groups calculated by the software, which was 24.83 ± 2.87 nm for the uACM film and 26.30 ± 2.93 nm for the donor cornea (Fig. 3C).

3.4. *In vitro biological properties*

The scanning electron microscopy showed that the subcultured HCECs could adhere and grow on the surface of the uACM film, but compared with the normal human corneal endothelial surface, the volume increased, the shape changed to fibroblast-like, and the intercellular connection was not tight enough. The subcultured RCECs can adhere and grow healthy on the surface of the uACM film and have a hexagonal shape and volume similar to that of the normal rabbit corneal endothelial surface (Fig. 4A). Immunofluorescence staining showed that the endothelial pump functional protein Na^+/K^+-ATPase and tight junction protein ZO-1 were positively expressed on the surface of human corneal endothelial grafts and rabbit corneal endothelial grafts (Fig. 4B).

3.5. *Transplantation of uACM films into rabbit corneas*

To evaluate whether the corneal endothelial graft constructed with uACM film can play a role in treating corneal endothelial dysfunction in vivo, we implanted the three groups into the rabbit corneal endothelial dysfunction model through DMEK surgery (Fig. 5A). The main steps of the surgical procedure are shown in Fig. 5B. Live-dead staining of the uACM with RCECs grafts showed that no cell growth was seen at the O-ring location and linear folds, and a small clump of dead cells was seen at the microscopic forceps contact. More importantly, RCECs were seen to be viable and evenly distributed in the uACM film (Fig. 5C). Under the slit-lamp observation of the uACM with RCECs transplanted eyes, the corneal transparency was decreased on day 4, while increased on week 1 and nearly recovered on week 2. The transparent corneal area corresponded to the endothelial graft area, and the opacity haze was seen on the border of the endothelial graft and the peripheral residual cornea. Throughout the follow-up, the uACM with RCECs endothelial implants adhered well to the posterior surface of the stroma, and no corneal neovascularization or anterior chamber inflammatory reaction was observed (Fig. 6A, left column). However, the uACM without RCECs transplanted eyes and the Descemetorhexis eyes have persistent corneal

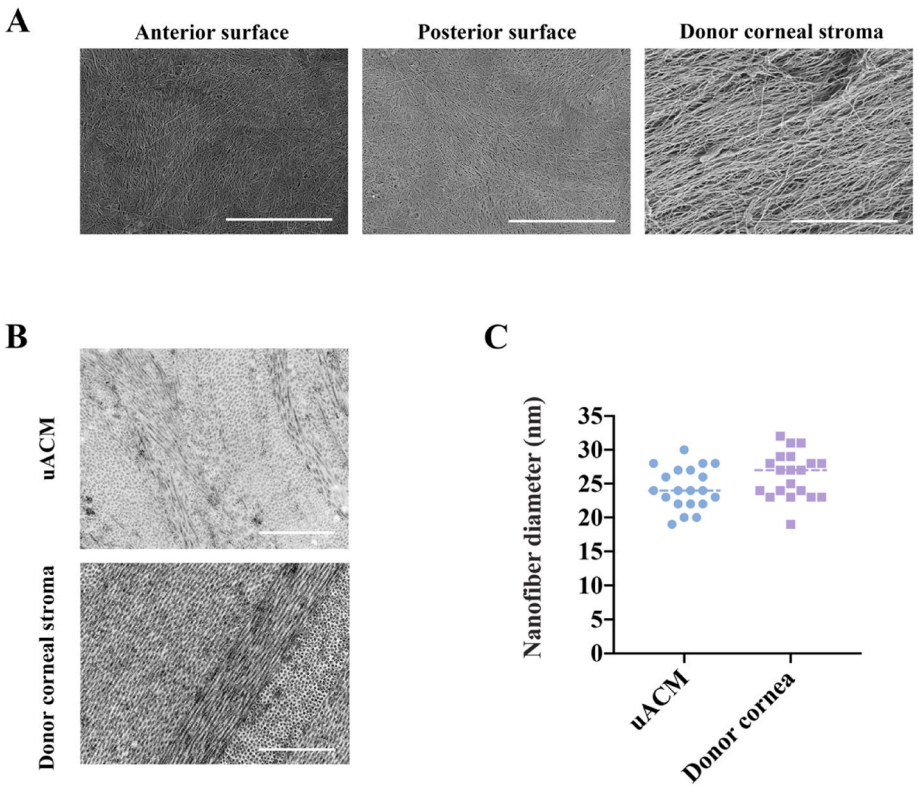

Fig. 3. Microstructural Characterization of the uACM. (A) Scanning electron microscopy of uACM films and donor corneal stromal layer. Scale bar = 5 μm. (B) The collagen fiber structure of uACM films and donor corneal stroma in transmission electron microscopy. Scale bar = 1 μm. (C) Comparison of collagen fibers diameter between uACM films and donor corneal stroma.

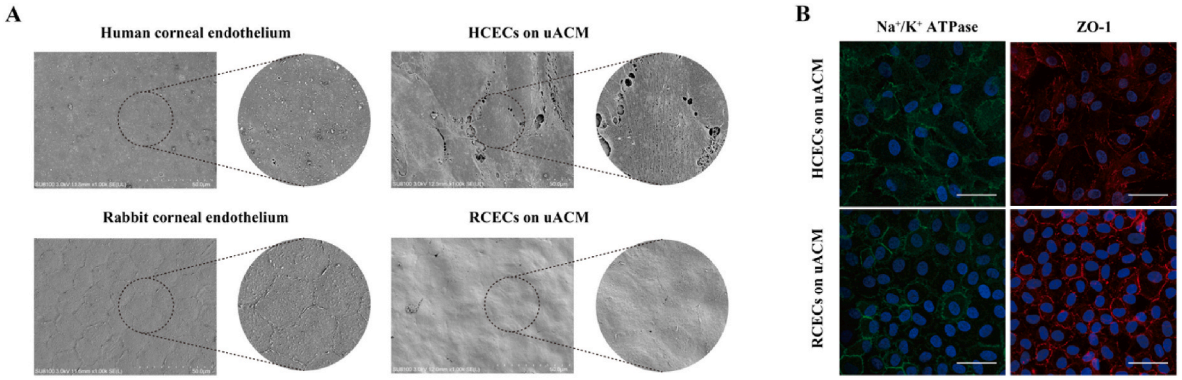

Fig. 4. Monolayer formation of HCECs and RCECs on the uACM. (A) Scanning electron microscopy of the human corneal endothelium, HCECs on uACM, rabbit corneal endothelium, and RCECs on uACM. (B) Immunofluorescence staining of HCECs on uACM, and RCECs on uACM. Na^+/K^+-ATPase, green; ZO-1, red.

edema and haze (Fig. 6A, center and right column). The corneal clarity score was presented in Fig. 6B. The changing trend of CCT determined by AS-OCT was consistent with the transparency score, and the CCT had recovered to the preoperative level in 4th week postoperatively (Fig. 7). Moreover, there was no significant difference in the central corneal endothelial cell density between the uACM with RCECs transplanted eyes and the normal contralateral eyes (Fig. 8A). Corneal topography of the uACM with RCECs transplanted eyes and their normal contralateral eyes at postoperative week 4 showed that the corneal thickness of the uACM with RCECs transplanted area was significantly lower than the peripheral area, and was similar to that of their normal contralateral eyes (Fig. 8B). Histological staining showed that the uACM with RCECs graft adhered well to the posterior surface of the rabbit corneal stroma, and no inflammatory reaction was observed between the uACM film and surrounding tissues. Endothelial cells grow as a monolayer on the posterior surface of uACM film and express ion pump functional protein Na^+/K^+-ATPase, tight junction protein ZO-1, and N-Cadherin. RCECs grew uniformly on the surface of uACM film and maintained their normal morphology and function in vivo. In addition, no endothelial cell was observed in the uACM without RCECs transplanted eyes and the Descemetorhexis eyes (Fig. 9A). Diffuse fibroblastic cell was seen in the junction area of the uACM with RCECs transplantation area and the residual endothelium of the peripheral recipient cornea, whereas endothelial cells with regular morphology were uniformly distributed in the uACM with RCECs transplantation area and the peripheral residual cornea (Fig. 9B).

4. Discussion

Corneal disease is one of the leading blinding diseases and is often

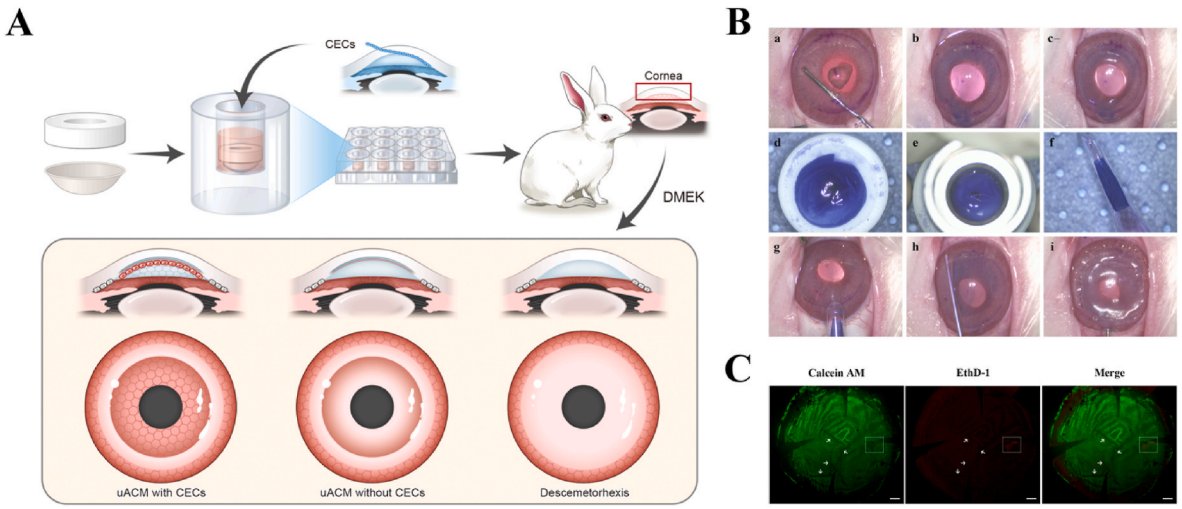

Fig. 5. In vivo experiments of uACM with RCECs graft implantation in the rabbit corneal endothelial dysfunction model through DMEK surgery. (A) Schematics of the in-vitro construction and in-vivo animal experiments of the bioengineered corneal endothelial grafts. (B) DMEK procedure performed on live rabbit corneas. Stripping of the Descemet's membrane and endothelium of the rabbit cornea with a diameter of 10 mm (a). Trypan blue staining confirmed no residual Descemet's membrane and endothelium remains in the stripped area (b). Anterior chamber injection of sterile air (c). Trypan Blue staining was applied to the endothelial implants, and subsequent identification of the endothelial surface was conducted by observing the pre-marked edge (d). The endothelial implant was cut with an 8-mm trephine (e). The endothelial implant was curled and transferred into an DMEK injector cartridge (f). The endothelial implant was inserted into the anterior chamber (g). Flattening and positioning the endothelial implant in the central area (h). Attaching the endothelial implant with air bubble (i). (C) Live-dead cell staining of the uACM with RCECs graft.

caused by endothelial dysfunction. The global scarcity of donor corneas has become the most important factor limiting the widespread application of corneal endothelial transplantation. Previously, we have fabricated cross-linked ACM scaffolds capable of generating high-quality corneal stromal implants suitable for transplantation, exhibiting favorable strength and deficient elasticity [17]. However, it is important to note that thick and rigid ACM scaffolds may be unsuitable for corneal endothelial keratoplasty, as this procedure necessitates thin and soft grafts resembling the human Descemet's membrane. Here we explored the utilization of an ultrathin and uncross-linked uACM film as a scaffold for tissue-engineered corneal endothelium. The main results of this study indicated that: (1) The uACM was an ultrathin and curved cornea-shaped film, which showed excellent optical and mechanical properties. (2) The uACM film was highly biomimetic to human Descemet's membrane regarding its histology, microstructure, and composition. (3) HCECs and RCECs have the capability to adhere and proliferate as a monolayer on the surface of the uACM films, thereby exhibiting distinctive endothelial markers of the endothelial cell. (4) The uACM with RCECs graft can be successfully implanted into the rabbit corneal endothelial dysfunction model through DMEK surgery, and it effectively retains its functionality in vivo.

The primary considerations for the fabrication of a corneal endothelial graft involve the thinness and curved shape of the cornea, as these factors are crucial for ensuring proper adherence of the implants to the posterior corneal surface and the restoration of visual acuity. Typically, the thickness of a DSEK graft ranges from 100 to 200 μm, whereas the thickness of Descemet's membrane in healthy adults is only 10–12 μm. The increased corneal thickness resulting from the graft can lead to postoperative farsightedness. On the other hand, a DMEK graft solely replaces the diseased Descemet's membrane and the endothelium, thereby achieving a complete anatomical and functional restoration [11,24]. By adjusting the concentration and volume of the decellularized corneal suspension, the dry uACM film thickness was regulated at 7.27 ± 1.20 μm, and the pre-wet uACM film thickness was regulated at 20.20 ± 2.52 μm, resembling the thickness of human Descemet's membrane. Yoshida et al. reported that the cornea-curved membrane could be affixed to the stromal layer's posterior surface, while the flat membrane could not. We utilized a spherical mold with an 8 mm curvature radius to fabricate uACM films, referring to the mold data by Yoshida et al. [65].

The poor transparency of the dry uACM film can be attributed to the refraction and diffuse reflection caused by the irregular collagen fibers. However, when the uACM film is saturated, it exhibits excellent optical properties. Additionally, the elongation at break increases while the tensile strength and Young's modulus decrease significantly. Consequently, the dry state is utilized for preservation and transportation purposes, while the pre-wet form is employed for in vitro reconstruction. Previous studies have reported that the mechanical properties of human Descemet's membrane [23]. Through a comparison of the mechanical properties between the pre-wet uACM film and the human Descemet's membrane, it is observed that the pre-wet uACM film demonstrates a reasonable elongation rate and weak tensile strength. Further investigation is necessary to explore the feasibility of utilizing the uACM film with weak tensile strength for endothelial scaffold, despite its limited involvement in clipping operations during in vitro reconstruction and in vivo transplantation. Additionally, the film exhibits superior stretching capabilities compared to Descemet's membrane, facilitating its easier flattening and fixation onto the posterior surface of the corneal stroma.

Referring to the architecture and functionality of the human Descemet's membrane, the convex anterior surface of the uACM film was utilized for adherence to the recipient corneal stroma following in vivo implantation, while the concave posterior surface of the uACM film was employed for the cultivation of a monolayer of the corneal endothelium. The human corneal Descemet's membrane is the basement membrane of endothelial cells, secreted by endothelial cells and composed of smooth and uniform amorphous structure [25,26]. The scanning electron microscopy results showed that the anterior and posterior surfaces of the uACM film had a collagen fiber structure similar to that of the donor corneal stroma, but the collagen fibers were more tightly connected and less regularly distributed [27,28]. The transmission electron microscopy results showed that the structure of collagen fiber arrangement in the cross-section of uACM film was similar to that of the donor corneal stroma. The transparency of uACM films is intricately linked to the diameter of collagen fibers and the spacing between these fibers. The remarkable transparency exhibited by uACM films can be attributed to the comparable diameter of collagen fibers present in the film and those found in the donor corneal stroma [29,30]. It is worth mentioning that

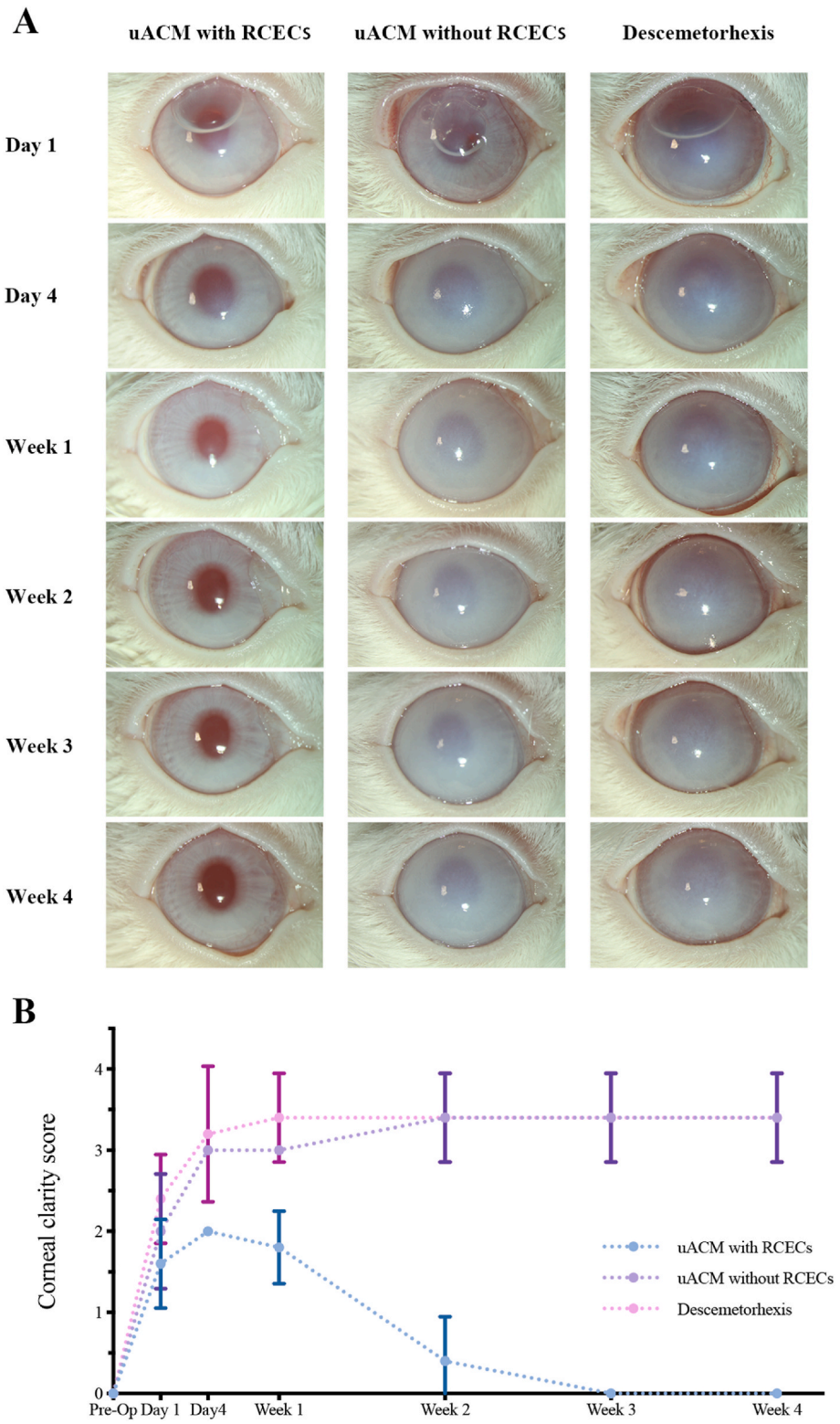

Fig. 6. Slit-lamp observation (A) and corneal transparency score change (B) in the rabbit corneal endothelial dysfunction model.

the processed discarded human corneal tissues preserve a variety of natural human corneal extracellular matrix components that do not exist in other natural or synthetic materials, thus realizing the compositional biomimetic reconstruction of native human corneal tissue. Masson staining was performed to detect collagen, PAS staining to detect glycoproteins, and Alcian blue staining to detect glycosaminoglycans [31]. Our results showed uACM film retains collagen, glycoproteins, and glycosaminoglycans well. Furthermore, we used the mass spectrometry iTRAQ method to quantitatively analyze the relative expression of proteins in the native human cornea and uACM film. The GO subcellular localization analysis found that most of the significantly down-regulated proteins were cellular components. Moreover, various types of collagens, fibronectin, and laminin in the extracellular matrix of donor cornea were well preserved. Decellularization of the donor corneal

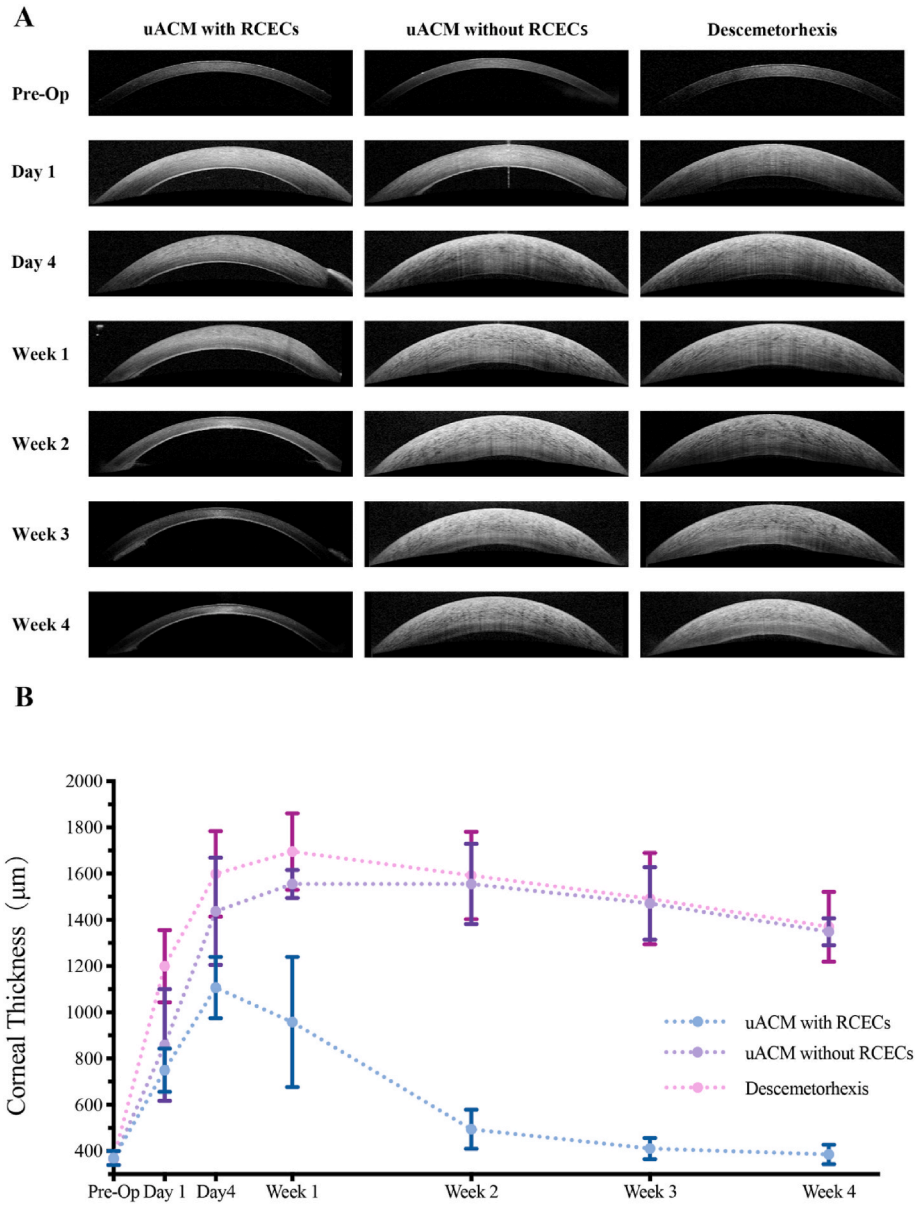

Fig. 7. AS-OCT images (A) and central corneal thickness change (B) in the rabbit corneal endothelial dysfunction model.

tissues can reduce the rate of corneal graft rejection [32].

In order to obtain a sufficient quantity of corneal endothelial cells, it is necessary to expand the cells in vitro. We conducted passaging and expansion of HCECs and RCECs in vitro, followed by inoculation on the surface of a film and subsequent detection of morphological and functional markers of endothelial cells. In this study, we observed that RCECs maintained a hexagonal morphology, while HCECs experienced endothelial-to-mesenchymal transition with increasing passages. The second or third generations of HCECs and RCECs were inoculated on the surface of uACM film to construct bioengineered corneal endothelial grafts in vitro. HCECs have the ability to adhere and proliferate on the surface of uACM film, while also expressing the endothelial pump functional protein Na^+/K^+-ATPase and the tight junction protein ZO-1. Following passaging, HCECs exhibited an observable increase in size, a morphological transformation towards a fibroblast-like appearance, and inadequate intercellular junctions. The restricted cell density of the bioengineered corneal endothelium, resulting from contact inhibition, may lead to a compromised mechanical barrier and ion pump function in vivo. Therefore, it remains necessary to conduct further research to determine whether the functionality of subcultured HCECs can be restored following implantation in vivo [33,34]. The extracellular matrix components present in Descemet's membrane, including Type IV collagen, laminin-511, and laminin-521 and fibronectin, have been observed to promote stimulate the adhesion and proliferation of human corneal endothelial cells [35–38]. In further research, we will try to use the above natural ingredients to modify the uACM film to study whether the adhesion, migration and proliferation of HCECs can be promoted in vitro construction. In our present study, RCECs maintained hexagonal endothelial cell morphology with tight intercellular junctions as the number of passages increased. The subcultured RCECs exhibited the capacity to adhere and proliferate on the surface of the uACM film, displaying a hexagonal morphology similar to that observed in the normal rabbit corneal endothelium. These cells formed tight connections, resulting in the formation of a complete endothelial layer. Immunohistochemical analysis revealed positive expression of the endothelial pump functional protein Na^+/K^+-ATPase and the tight junction protein ZO-1 on the surface of the rabbit corneal endothelial grafts. Through the in vitro construction process, we successfully prepared rabbit corneal endothelial grafts with healthy endothelial cell morphology and function, which will be further investigated in an in

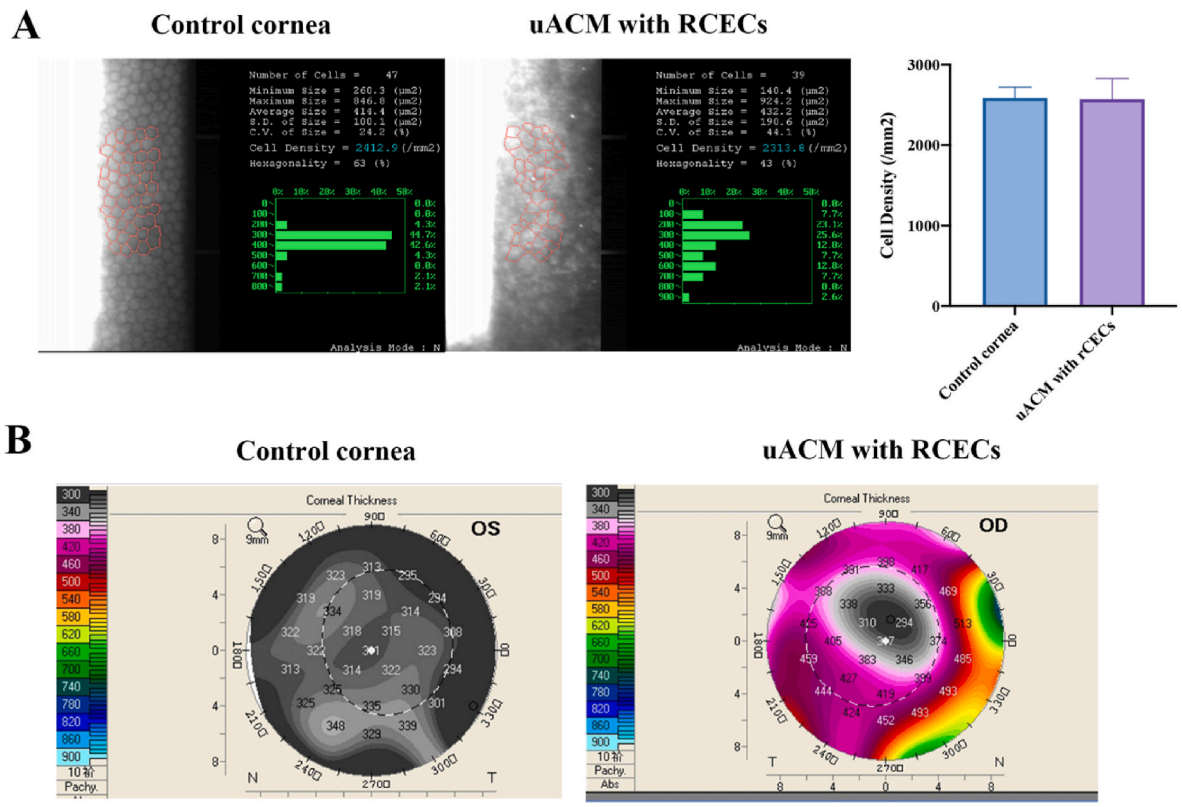

Fig. 8. The corneal endothelial cell density (A) and corneal topography (B) after the uACM with RCECs graft implantation at the fourth week postoperatively.

vivo study.

In order to examine the in vivo safety and efficacy, the bioengineered corneal endothelial grafts, which were constructed using uACM films and RCECs, were surgically implanted into a rabbit model with corneal endothelial dysfunction through DMEK surgery. The rabbit model was created by mechanically dissecting Descemet's membrane and endothelial layer with a diameter exceeding 10 mm in the central cornea. There was a margin area between the uACM with RCECs grafts (8-mm diameter) and the scraped area (10-mm diameter), resulting in a temporary decrease in corneal transparency at the fourth postoperative day. However, transparency gradually improved over the course of the first postoperative week and fully recovered by the second postoperative week. The changing trend of CCT measured by AS-OCT was consistent with the transparency score, and the CCT in the fourth postoperative week has been restored to the preoperative level. These results indicate that uACM with RCECs grafts can preserve corneal transparency and maintain standard corneal thickness in vivo. Moreover, there was no significant difference in the corneal endothelial cell density between the transplanted and normal contralateral eyes. Histological staining revealed the complete removal of Descemet's membrane, successful adherence of the uACM with RCECs graft to the posterior surface of the rabbit corneal stroma, and absence of any inflammatory reaction. Furthermore, the RCECs exhibited uniform growth as a monolayer on the posterior surface of the uACM film, while retaining their normal morphology and functional markers in vivo. Significantly, our study demonstrates that the restoration of corneal transparency and CCT in the uACM with RCECs transplantation group is primarily attributed to the swift reaction of endothelial cells within the transplanted endothelial grafts, rather than the proliferation and migration of autologous endothelial cells, as evidenced by the 4-week follow-up period. Firstly, the uACM without RCECs transplantation group and the Descemetorhexis group exhibited persistent corneal opacity and edema, which was further confirmed by histological staining revealing the absence of cells on the posterior corneal surface and negative expression of corneal endothelial cell markers. Secondly, corneal topography results showed that the corneal thickness of the uACM with RCECs implanted eyes in the transplanted area with a diameter of about 8 mm was significantly lower than that of the surrounding area. Finally, SEM results demonstrated the presence of diffuse fibrotic cells between the uACM with RCECs transplanted area's endothelial cells and the distribution junction of residual corneal endothelial cells in the periphery. The utilization of a uACM film-based bioengineered corneal endothelial graft in DMEK surgery proved successful in treating rabbit corneal endothelial dysfunction models. A long-term follow-up is still needed to observe its long-term effects. HCECs have demonstrated the ability to adhere and proliferate on film surfaces while expressing their characteristic markers, albeit with sub-optimal morphology. Therefore, there is currently a lack of animal experimental studies involving HCECs. Nevertheless, our research serves as a foundation for future investigations into bioengineered grafts for human corneal endothelial transplantation.

The selection of an appropriate surgical technique is of utmost importance in advancing the utilization of biomaterials in future clinical settings. This research demonstrates that the uACM film possesses the ability to withstand routine clamping operations during cell culture and surgical procedures, thereby validating its favorable mechanical characteristics. Furthermore, the bioengineered endothelial grafts can be conveniently curled within the DMEK endothelial injector using the appropriate suction pressure in a corneal storage medium and subsequently implanted into the anterior chamber with the suitable bolus pressure. The flattening, position adjustment, and graft fixation procedures are executed without direct contact to safeguard the integrity of the endothelial cells [39,40]. By utilizing existing DMEK surgical instruments and techniques, there is no need to develop novel grafting methods to accommodate the grafts. This study presents a novel strategy for the reconstruction of tissue-engineered corneal endothelium, which holds immense importance in mitigating the scarcity of donor corneas.

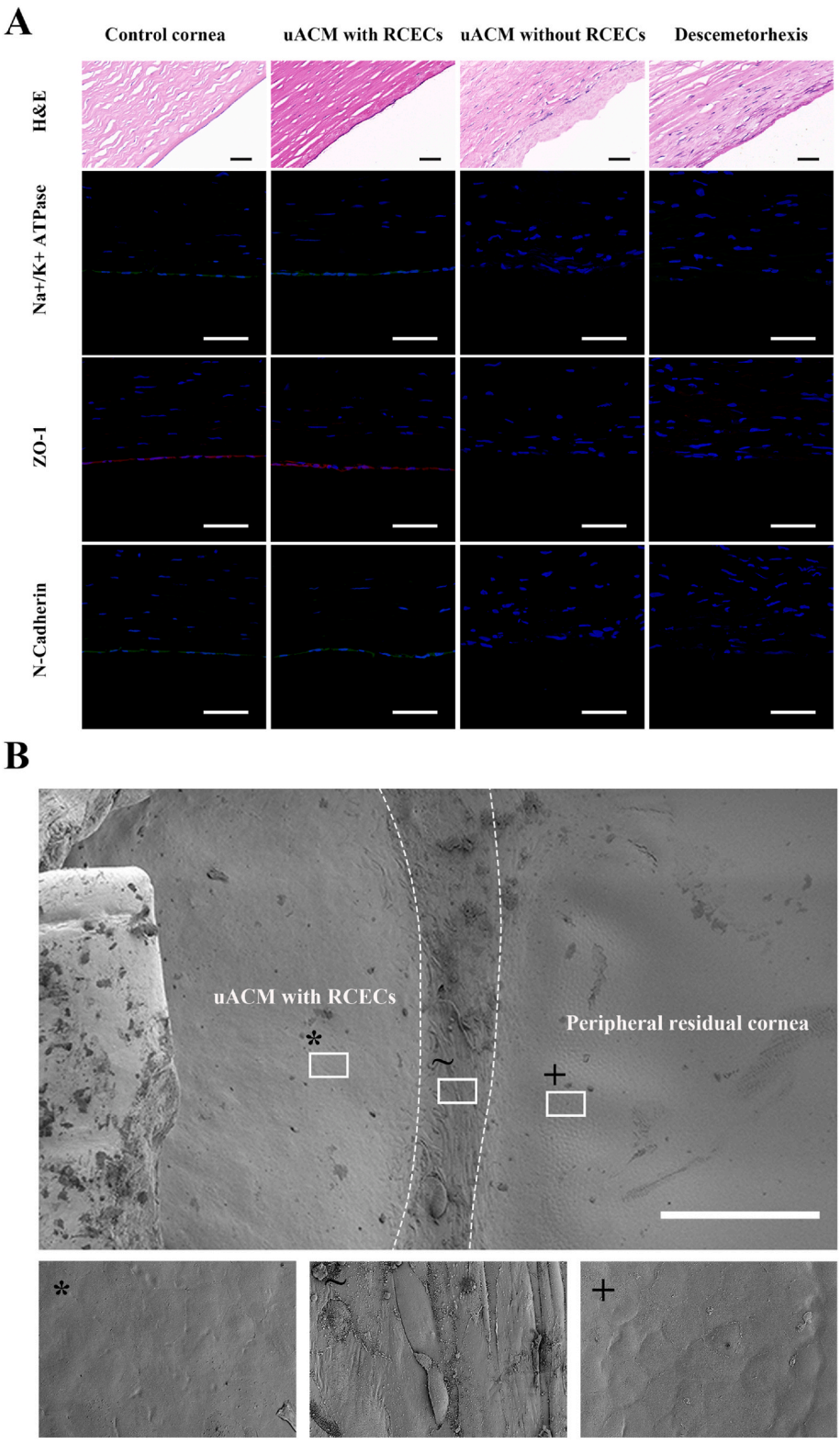

Fig. 9. Histological and structural analyses in the rabbit corneal endothelial dysfunction model at four weeks after surgery. (A) HE staining and immunofluorescence staining of the uACM with RCECs transplanted eyes, uACM without RCECs transplanted eyes, Descemetorhexis eyes, and normal rabbit eyes. Scale bar = 50 μm. Na^+/K^+-ATPase, green; ZO-1, red; N-Cadherin, green. (B) SEM observation of the uACM with RCECs transplanted eyes. Scale bar = 50 μm.

5. Conclusions

The uACM films were generated by remodeling of decellularized corneal tissue to achieve biomimetics properties in both composition and structure. HCECs and RCECs were observed to proliferate on the surface of uACM films, exhibiting the expression of their respective characteristic markers. The utilization of uACM film and RCECs in the construction of bioengineered corneal endothelial grafts enabled the treatment of rabbit corneal endothelial dysfunction models through DMEK surgery. Consequently, our study showcases the potential of

uACM film in the fabrication of bioengineered corneal endothelium, offering a novel approach to corneal endothelial reconstruction.

CRediT authorship contribution statement

Lijie Xie: Writing – original draft, Methodology, Funding acquisition, Data curation, Conceptualization. **Xiaojuan Dong:** Writing – review & editing, Supervision, Methodology, Investigation, Data curation. **Jianping Ji:** Supervision, Data curation. **Chen Ouyang:** Methodology, Data curation. **Jing Wu:** Methodology, Investigation. **Chao Hou:** Methodology. **Ting Huang:** Writing – review & editing, Supervision, Funding acquisition, Conceptualization.

Declaration of competing interest

The authors declare that they have no known competing financial interests or personal relationships that could have appeared to influence the work reported in this paper.

Data availability

Data will be made available on request.

Acknowledgements

The authors acknowledge financial support from the National Natural Science Foundation of China (Grant No. 81870628) and the NSFC Incubation Project of Guangdong Provincial People's Hospital (Grant No. KY0120220056).

References

[1] J.S. Singh, T.A. Haroldson, S.P. Patel, Characteristics of the low density corneal endothelial monolayer, Exp. Eye Res. 115 (2013) 239–245.
[2] J. Hollingsworth, I. Perez-Gomez, H.A. Mutalib, N. Efron, A population study of the normal cornea using an in vivo, slit-scanning confocal microscope, Optom. Vis. Sci. 78 (10) (2001) 706–711.
[3] H.F. Edelhauser, The resiliency of the corneal endothelium to refractive and intraocular surgery, Cornea 19 (3) (2000) 263–273.
[4] D.T.H. Tan, J.K.G. Dart, E.J. Holland, S. Kinoshita, Corneal transplantation, Lancet 379 (9827) (2012) 1749–1761.
[5] K. Webb, C. Dun, X. Dai, A. Chen, D. Srikumaran, M.A. Makary, F.A. Woreta, Trends of surgery, Patient, and Surgeon characteristics for corneal Transplants in the Medicare population from 2011 to 2020, Cornea (2024).
[6] P. Ple-Plakon, R. Shtein, Trends in corneal transplantation: indications and techniques, Curr. Opin. Ophthalmol. 25 (4) (2014) 300–305.
[7] M.O. Price, M. Gorovoy, B.A. Benetz, F.W. Price Jr., H.J. Menegay, S.M. Debanne, J.H. Lass, Descemet's stripping automated endothelial keratoplasty outcomes compared with penetrating keratoplasty from the Cornea Donor Study, Ophthalmology 117 (3) (2010) 438–444.
[8] D. Tan, J. Dart, E. Holland, S. Kinoshita, Corneal transplantation, Lancet (London, England) 379 (9827) (2012) 1749–1761.
[9] P. Gain, R. Jullienne, Z. He, M. Aldossary, S. Acquart, F. Cognasse, G. Thuret, Global Survey of corneal transplantation and eye banking, JAMA ophthalmology 134 (2) (2016) 167–173.
[10] G. Melles, Posterior lamellar keratoplasty: DLEK to DSEK to DMEK, Cornea 25 (8) (2006) 879–881.
[11] S. Deng, W. Lee, K. Hammersmith, A. Kuo, J. Li, J. Shen, M. Weikert, R. Shtein, Descemet membrane endothelial keratoplasty: safety and outcomes: a report by the American academy of Ophthalmology, Ophthalmology 125 (2) (2018) 295–310.
[12] L. Baydoun, I. Vasiliauskaite, S. Luceri, M.J. Jager, S.C. Schaal, V. Bourgonje, S. Oellerich, G.R.J. Melles, Long-term outcome after bilateral DMEK for fuchs endothelial corneal dystrophy, Cornea (2023).
[13] J.Y. Lai, K.H. Chen, W.M. Hsu, G.H. Hsiue, Y.H. Lee, Bioengineered human corneal endothelium for transplantation, Arch. Ophthalmol. 124 (10) (2006) 1441–1448.
[14] G.H. Hsiue, J.Y. Lai, K.H. Chen, W.M. Hsu, A novel strategy for corneal endothelial reconstruction with a bioengineered cell sheet, Transplantation 81 (3) (2006) 473–476.
[15] J.Y. Lai, K.H. Chen, G.H. Hsiue, Tissue-engineered human corneal endothelial cell sheet transplantation in a rabbit model using functional biomaterials, Transplantation 84 (10) (2007) 1222–1232.
[16] T.M. Tran, J.H. Hou, Clinical applications of bioengineered tissue-cellular products for management of corneal diseases, Curr. Opin. Ophthalmol. 34 (4) (2023) 311–323.
[17] L. Xie, C. Ouyang, J. Ji, J. Wu, X. Dong, C. Hou, T. Huang, Construction of bioengineered corneal stromal implants using an allogeneic cornea-derived matrix, Mater. Sci. Eng., C 120 (2021) 111673.
[18] Z. Han, J. Sun, Y. Zhang, F. He, Y. Xu, K. Matsumura, L.S. He, J.W. Qiu, S.H. Qi, P. Y. Qian, iTRAQ-based proteomic profiling of the barnacle Balanus amphitrite in response to the antifouling compound meleagrin, J. Proteome Res. 12 (5) (2013) 2090–2100.
[19] B. Wen, R. Zhou, Q. Feng, Q. Wang, J. Wang, S. Liu, IQuant: an automated pipeline for quantitative proteomics based upon isobaric tags, Proteomics 14 (20) (2014) 2280–2285.
[20] S. Wahlig, G.S.L. Peh, K. Adnan, H.P. Ang, C.N. Lwin, F. Morales-Wong, H.S. Ong, M. Lovatt, J.S. Mehta, Optimisation of storage and transportation conditions of cultured corneal endothelial cells for cell replacement therapy, Sci. Rep. 10 (1) (2020) 1681.
[21] G.S.L. Peh, H.P. Ang, C.N. Lwin, K. Adnan, B.L. George, X.Y. Seah, S.J. Lin, M. Bhogal, Y.C. Liu, D.T. Tan, J.S. Mehta, Regulatory compliant tissue-engineered human corneal endothelial grafts restore corneal function of rabbits with bullous keratopathy, Sci. Rep. 7 (1) (2017) 14149.
[22] C. Zhang, L. Du, P. Sun, L. Shen, J. Zhu, K. Pang, X. Wu, Construction of tissue-engineered full-thickness cornea substitute using limbal epithelial cell-like and corneal endothelial cell-like cells derived from human embryonic stem cells, Biomaterials 124 (2017) 180–194.
[23] B. Ozcelik, K.D. Brown, A. Blencowe, K. Ladewig, G.W. Stevens, J.P. Scheerlinck, K. Abberton, M. Daniell, G.G. Qiao, Biodegradable and biocompatible poly (ethylene glycol)-based hydrogel films for the regeneration of corneal endothelium, Adv. Healthcare Mater. 3 (9) (2014) 1496–1507.
[24] R. de Oliveira, S. Wilson, Descemet's membrane development, structure, function and regeneration, Exp. Eye Res. 197 (2020) 108090.
[25] D. Xia, S. Zhang, E. Nielsen, A. Ivarsen, C. Liang, Q. Li, K. Thomsen, J. Hjortdal, M. Dong, The ultrastructures and mechanical properties of the descement's membrane in fuchs endothelial corneal dystrophy, Sci. Rep. 6 (2016) 23096.
[26] D.W. DelMonte, T. Kim, Anatomy and physiology of the cornea, J. Cataract Refract. Surg. 37 (3) (2011) 588–598.
[27] J.S. Choi, J.K. Williams, M. Greven, K.A. Walter, P.W. Laber, G. Khang, S. Soker, Bioengineering endothelialized neo-corneas using donor-derived corneal endothelial cells and decellularized corneal stroma, Biomaterials 31 (26) (2010) 6738–6745.
[28] M.A. Shafiq, R.A. Gemeinhart, B.Y. Yue, A.R. Djalilian, Decellularized human cornea for reconstructing the corneal epithelium and anterior stroma, Tissue Eng. C Methods 18 (5) (2012) 340–348.
[29] Y. Tanaka, K. Baba, T.J. Duncan, A. Kubota, T. Asahi, A.J. Quantock, M. Yamato, T. Okano, K. Nishida, Transparent, tough collagen laminates prepared by oriented flow casting, multi-cyclic vitrification and chemical cross-linking, Biomaterials 32 (13) (2011) 3358–3366.
[30] D.W. DelMonte, T. Kim, Anatomy and physiology of the cornea, J. Cataract Refract. Surg. 37 (3) (2011) 588–598.
[31] G. Yam, N. Yusoff, T. Goh, M. Setiawan, X. Lee, Y. Liu, J. Mehta, Decellularization of human stromal refractive lenticules for corneal tissue engineering, Sci. Rep. 6 (2016) 26339.
[32] S. Wilson, L. Sidney, S. Dunphy, H. Dua, A. Hopkinson, Corneal decellularization: a method of recycling unsuitable donor tissue for clinical translation? Curr. Eye Res. 41 (6) (2016) 769–782.
[33] N. Joyce, Proliferative capacity of the corneal endothelium, Prog. Retin. Eye Res. 22 (3) (2003) 359–389.
[34] B. Aboalchamat, K. Engelmann, M. Böhnke, P. Eggli, J. Bednarz, Morphological and functional analysis of immortalized human corneal endothelial cells after transplantation, Exp. Eye Res. 69 (5) (1999) 547–553.
[35] P.W. Madden, J.N. Lai, K.A. George, T. Giovenco, D.G. Harkin, T.V. Chirila, Human corneal endothelial cell growth on a silk fibroin membrane, Biomaterials 32 (17) (2011) 4076–4084.
[36] R. Palchesko, K. Lathrop, J. Funderburgh, A. Feinberg, In vitro expansion of corneal endothelial cells on biomimetic substrates, Sci. Rep. 5 (2015) 7955.
[37] N. Okumura, K. Kakutani, R. Numata, M. Nakahara, U. Schlötzer-Schrehardt, F. Kruse, S. Kinoshita, N. Koizumi, Laminin-511 and -521 enable efficient in vitro expansion of human corneal endothelial cells, Invest. Ophthalmol. Vis. Sci. 56 (5) (2015) 2933–2942.
[38] Y.J. Hsueh, D.H. Ma, K.S. Ma, T.K. Wang, C.H. Chou, C.C. Lin, M.C. Huang, L. J. Luo, J.Y. Lai, H.C. Chen, Extracellular matrix protein coating of processed fish scales improves human corneal endothelial cell adhesion and proliferation, Transl Vis Sci Technol 8 (3) (2019) 27.
[39] G. Melles, T. Ong, B. Ververs, J. van der Wees, Descemet membrane endothelial keratoplasty (DMEK), Cornea 25 (8) (2006) 987–990.
[40] N. Gupta, A. Kumar, P.K. Vaddavalli, N.R. Mahapatra, A. Varshney, P. Ghosh, Efficient reduction of the scrolling of Descemet membrane endothelial keratoplasty grafts by engineering the medium, Acta Biomater. 171 (2023) 239–248.